Revista Mexicana de Ingeniería Química
ISSN: 1665-2738
amidiq@xanum.uam.mx
Universidad Autónoma Metropolitana
Unidad Iztapalapa
México

Corral-Escárcega, M.C.; Ruiz-Gutiérrez, M.G.; Quintero-Ramos, A.; Meléndez-Pizarro, C.O.; Lardizabal-Gutiérrez, D.; Campos-Venegas, K.
USE OF BIOMASS-DERIVED FROM PECAN NUT HUSKS (Carya illinoinensis) FORCHROMIUM REMOVAL FROM AQUEOUS SOLUTIONS. COLUMN MODELING AND ADSORPTION KINETICS STUDIES
Revista Mexicana de Ingeniería Química, vol. 16, núm. 3, 2017, pp. 939-953
Universidad Autónoma Metropolitana Unidad Iztapalapa
Distrito Federal, México

Vol. 16, No. 3 (2017) 939-953
Revista Mexicana de Ingeniería Química

USE OF BIOMASS-DERIVED FROM PECAN NUT HUSKS (*Carya illinoinensis*) FOR CHROMIUM REMOVAL FROM AQUEOUS SOLUTIONS. COLUMN MODELING AND ADSORPTION KINETICS STUDIES

USO DE BIOMASA DERIVADA DEL PERICARPIO DE NUEZ PECANERA (*Carya illinoinensis*) PARA LA REMOCIÓN DE CROMO DE SOLUCIONES ACUOSAS. MODELACIÓN EN COLUMNA Y ESTUDIOS DE CINÉTICAS DE ADSORCIÓN

M.C. Corral-Escárcega[1], M.G. Ruiz-Gutiérrez[1], A. Quintero-Ramos[1], C.O. Meléndez-Pizarro[1]*, D. Lardizabal-Gutiérrez[2], K. Campos-Venegas[2]

[1] *Facultad de Ciencias Químicas. Universidad Autónoma de Chihuahua. Circuito Universitario s/n. Campus Universitario No.2. Chihuahua, Chihuahua México. C.P. 31125.*

[2] *Centro de Investigación en Materiales Avanzados, S. C. Avenida Miguel de Cervantes 120 Complejo Industrial Chihuahua, Chihuahua, Chihuahua, México.*

Received March 4, 2017; Accepted May 12, 2017

Abstract

Chromium (VI) removal from water was studied using two varieties of pecan nut husks (PNHs): Barton and Native. Influent Cr(VI) solutions at different pH values (2.5 and 6.18) and particle sizes (0.42 and 0.85 mm) were performed. Both PNH varieties showed reduction to Cr(III) and adsorption of Cr(VI) and Cr(III). The Thomas model adequately (R^2 of 0.79-0.94) describes the Cr(VI) adsorption for Barton PNH. Microscopy studies of PNH morphology showed some morphological changes attributed to chromium retention. The Barton PNH variety presented a higher Cr(VI) absorption with a longer exhaustion time (15-30 min) for both particle sizes. Native PNH for both particle sizes with a pH of 6.18 had the highest concentrations at equilibrium but short exhaustion time (10-15 min). PNH could be a sustainable alternative material for the Cr(VI) removal from contaminated waters.

Keywords: pecan nut husk, biosorption, chromium, Thomas model, biomass.

Resumen

Se estudió la remoción de cromo (VI) en agua usando dos variedades diferentes de pericarpio de nuez pecanera (PNHs): Barton y Criolla. El afluente fue una solución de Cr(VI) con diferentes valores de pH (2.5 y 6.18) y dos diferentes tamaños de partícula (0.42 y 0.85). Ambas variedades de PNHs mostraron reducción a Cr(III) y adsorción de Cr(VI) y Cr(III). El modelo de Thomas describe adecuadamente (R^2 de 0.79-0.94) la adsorción de Cr(VI) para la variedad Barton de PNH. Estudios de microscopia de la variedad Barton de PNH presenta una alta adsorción de Cr(VI) en un tiempo de saturación largo (15-30 min) para ambos tamaños de partícula. Ambos tamaños de partícula del PNH de la variedad Criolla a pH de 6.18 tuvieron una alta concentración en el equilibrio y corto tiempo de saturación (10-15 min). El pericarpio de nuez pecanera pueden ser un material alternativo sostenible para la remoción de Cr(VI) en aguas contaminadas.

Palabras clave: cáscara de nuez, biosorción, cromo, modelo de Thomas, biomasa.

1 Introduction

Chromium (Cr), like other heavy metals, has been linked to industrialization and has been associated with environmental problems such as pollution. Some industrial activities related to Cr contamination are electroplating, steel and automobile manufacturing, leather tanning, metal processing, mining, and the production of paint pigments, dyes, cement, and textiles (Bielicka *et al*., 2005; Miretzky and Fernandez, 2010; Dhal *et al*., 2013; Paredes-Carrera *et al*., 2015). Groundwater and surface water can be contaminated with Cr by the discharge of untreated industrial wastewater (Owlad *et al*., 2009; Paredes-Carrera *et al*., 2015, Badillo-Camacho *et al*., 2016). Moreover, the dumping of solid industrial waste pollutes the soil, which can also contaminate groundwater with chromium compounds through lixiviation (Bielicka *et al*., 2005).

* *Corresponding author. E-mail*: cmelende@uach.mx

Environmental problems with Cr occur because Cr is not biodegradable, it bioacumulates in living organisms, and it is toxic (Barrera-Díaz *et al*., 2012).

The toxicity, solubility, and mobility of Cr depend on its oxidation state (Badillo-Camacho *et al*., 2016). Chromium in the Eh-pH range of natural water generally exists in two oxidation states: trivalent Cr(III) and hexavalent Cr(VI). On one hand, Cr(VI) is considered to be more toxic and is water soluble in the complete range of pH (Dhal *et al*., 2013). Moreover, Cr(VI) has a high mobility (Barrera-Díaz *et al*., 2012), which can cross biological membranes easily damaging DNA (McLean *et al*., 2012); therefore, Cr(VI) is considered a mutagenic and carcinogenic anion (Pechova and Pavlata, 2007; Paredes-Carrera *et al*., 2015). On the other hand, Cr(III) is a micronutrient essential for the metabolism of carbohydrates, lipids, and proteins in living organisms (Pechova and Pavlata, 2007), and it is a thousand times less toxic than Cr(VI) (Barrera-Díaz *et al*., 2012). The species $Cr(OH)^{2+}$, $Cr(OH)_3^0$, and $Cr(OH)_4^-$ prevail at low Eh, whereas, under oxidizing conditions, the species $HCrO_4^-$, CrO_4^{2-}, and $Cr_2O_7^{2-}$ are observed, depending on the pH of the Cr concentration (Owlad *et al*., 2009). In water, Cr(VI) is generally present as a soluble anion; therefore, the removal of Cr(VI) from wastewater is necessary before discharge due its toxicity to living organisms (McNeill *et al*., 2012).

Several methods have been used to remove Cr(VI) from aqueous effluents. Chemical precipitation, ionic exchange, oxidation-reduction, membrane filtration, coagulation, and adsorption are the most used technologies. The generation and disposal of solid waste are drawbacks of the precipitation and oxidation-reduction methods. Adsorption with activated carbon is considered to be one of the most effective methods for removing Cr(VI) from water (Li *et al*., 2012; Paredes-Carrera *et al*., 2015); however, the production of activated carbon is expensive (Owlad *et al*., 2009), and the use of membranes involves high operating costs. To overcome these disadvantages, biosorption has been proposed as a solution (Gadd, 2009) because it is inexpensive, the materials are readily available, and biosorption is more effective for metal removal than other physicochemical methods (Owlad *et al*., 2009).

The use of biosorbents, which are also known as green adsorbents (Kyzas and Kostoglou, 2014), has been extensively reported for removing Cr(VI) from aqueous solutions (Khan *et al*., 2004; Gardea-Torresdey *et al*., 2004; Demirbas, 2008;Owlad *et al*., 2009). Specifically, agro-waste biosorbents have been commonly employed in batch or column systems. Agro-wastes are lignocellulosic materials that have been reported in a raw or modified form, such as rice husks (Bansal *et al*., 2009), palm flowers (Elangovan *et al*., 2008a), maize cobs (Chen *et al*., 2012), olive pomace (El-Sheikh *et al*., 2011), straw and wheat bran (Farooq *et al*., 2010), saw dust (Bhattacharya *et al*., 2008), and walnut hulls (Wang *et al*., 2009), among others, and can be used to remove Cr (Aliabadi *et al*., 2006; Suresh, 2010; Chowdhury *et al*., 2013; Gautam *et al*., 2014). Another possible lignocellulosic material is the pericarp or husk of the pecan nut (*Carya illinoinensis*); this husk is a by-product of pecan nut production, which is commonly burned without an alternative use. Pecan nuts are widely cultivated in the southern and southwestern regions of the United States and in northern Mexico; these countries are the first and second largest world producers, respectively (Hadjigeorgalis *et al*., 2015). Though its use as a biosorbent for Cr(VI) has not been reported, pecan nut husks (PNHs) have been used in the removal of a dye and lead in aqueous solutions (Hernández-Montoya *et al*., 2011).

The bioadsorption of metals has been predicted through the use of mathematical models. Variables such as the flow rate, influent solution concentration, solid-liquid ratio, pH of the influent, particle size, and support composition have been considered because they are directly related with the behavior of metal removal kinetics. Thus, the application of predictive models using experimental data from breakthrough curves predict the dynamic behavior of the column in the removal of different metals, and these models have been developed for a wide variety of materials (Vijayaraghavan *et al*., 2005; Medvidović *et al*., 2007). Among these mathematical models are the Adams-Bohart, Yoon-Nelson, and Thomas models (Chu, 2004; Chen *et al*., 2012; Chowdhury *et al*., 2013), which have been reported for the removal of Cr(VI). The Thomas model is widely used, and it is the most general method for predicting column performance. Its application for the determination of some constants, which indicate the operation of the organic material support column for the removal of metals, is promising.

The aim of this research is to evaluate the use of the husks of two pecan nut (*Carya illinoinensis*) varieties at different particle sizes to remove Cr(VI) from aqueous solutions with different pH levels through a laboratory-scale fixed-bed column. Moreover, the biosorption process was predicted through Thomas model fitting to describe the performance of the

column in the adsorption of Cr(VI).

2 Materials and methods

2.1 Materials

Husks from the Barton and Native pecan nut (*Carya illinoinensis*) were obtained from Chihuahua, Mexico. All reagents were analytical grade and obtained from J.T. Baker (Mexico City, Mexico), except when noted. Stock solution (1000 mg/L) of Cr(VI) was prepared from $K_2Cr_2O_7$. The calibration curve for Cr(VI) as the influent (2.28 ± 0.1 mg/L) solution was prepared by appropriate dilution of the stock solution using deionized water. The initial pH (2.5 ± 0.02 and 6.18 ± 0.1) of the influent solutions was adjusted to the desired pH using diluted HNO_3 or NaOH, and a Hanna instrument pH meter was used (Woonsocket, RI, USA). The atomic absorption standard solution (Sigma-Aldrich, St. Louis, MO, USA) of 998 mg/L Cr(III) was used to prepare the calibration curve for total chromium quantification

2.2 Methods

2.2.1 Chromium concentration analysis

Hexavalent chromium was analyzed using a diphenylcarbazide method (APHA, 1975). The absorbance of the pink-colored complex was measured with a UV-Vis HACH DR/4000 spectrophotometer (Loveland CO, USA) at 540 nm. The concentration of total chromium was determined using a Perkin Elmer Aanalyst 700 atomic absorption spectrophotometer (Waltham, MA, USA) with an air-acetylene reducing flame at a wavelength of 357.9 nm and 0.7-nm slit width. A hollow cathode lamp was used. The concentration of trivalent chromium was determined as the difference between the total chromium and hexavalent chromium concentration.

2.2.2 Preparation of the PNH

The PNHs for each variety were treated separately; they were washed with distilled water to remove any foreign material and dried at 100°C in an oven (Fisher Scientific, 850G, Pittsburgh, PA, USA) for 24 h. The material was triturated using a domestic blender and sieved with a laboratory sieve shaker (Russell Finex Ltd., Middlesex, UK). Particle sizes of 0.42 mm and 0.85 mm were selected. A second wash with distilled water was performed, primarily to remove tannins. The material was oven-dried at 100°C until constant weight

2.2.3 Characterization

As part of the PNH characterization, a proximal analysis was performed for both PNH varieties. Moisture, total protein, total fat, fiber, and ash content were analyzed using the 1998 Association of Analytical Communities (AOAC) methods 950.02, 960.52, 920.39, 962.09, and 923.03, respectively (AOAC, 1998). Carbohydrates were calculated by difference. The point zero charge (pH_{pzc}) was determined according to a previously reported method (Kolsmulski, 2004). Capped test tubes with different PNH masses (0.05-0.55 g) and 10 mL of 0.1-M NaCl were agitated and allowed to equilibrate for 48 h with intermittent stirring. The final pH values were plotted against the PNH mass. The point where the pH remains constant gave pH_{pzc}. The total phenolic content was determined using the Folin-Ciocalteu method (Singleton *et al*., 1999) with some modifications. The PNHs (10 g) were extracted twice with 100 mL of methanol (50%) over 24 h. The extract (30 μL), deionized water (3 mL), and the Folin-Ciocalteu reagent (Sigma-Aldrich, St. Louis, MO, USA) were mixed and allowed to stand for 10 min. After neutralization with 600 μL of 20% sodium carbonate, the mixture was incubated for 20 min at 40°C in a water bath and cooled on ice. The absorbance was measured at 760 nm using a UV-Vis Lambda spectrophotometer (Perkin Elmer, Waltham, MA, USA), and a calibration curve of gallic acid (Sigma-Aldrich, St. Louis, MO, USA) was used. The results were expressed as milligrams of gallic acid equivalents per 100 g of sample (mg GAE/100 g). The quantification was performed in triplicate for each extract. Condensed tannins were quantified according to the Stiasny number method, which determines the reactivity of tannins to formaldehyde in an acid medium (Yazaky *et al*., 1993). Ten millilitres of the aqueous extraction with 10 mL of 38% aqueous formaldehyde and 5 mL 12-M HCl were heated under reflux for 30 min. The hot mixture was filtered using a sintered glass filter. The precipitate was dried to a constant weight. The Stiasny number is reported as a percentage of the weight of the precipitate to the weight of the starting sample. Thermogravimetric analysis (TGA) in air was achieved using TA Instruments calorimetry (Q-200, Crawley, England) with a program of 30 to 800°C and

a temperature ramp of 10°C/min.

The presence of functional groups in PNH was analyzed using a Perkin Elmer GX Fourier transform infrared spectrophotometer (FTIR; Waltham, MA, USA) in the range of 4000-600 cm^{-1}, equipped with an attenuated total reflectance (ATR) accessory. The ATR-FTIR analysis was not only achieved for Barton and Native PNH but also for the PNH used in the column experiments after the removal of Cr(VI); the samples were oven dried to remove moisture. To examine the morphological characteristics of the PNH before and after Cr(VI) sorption, scanning electron microscopy (SEM) was performed. A scanning electron microscope (JSM-5800LV, JEOL, Akishima, Japan) was used at acceleration rate of 15 kV. The SEM was equipped with dispersive X-ray (EDX) detector.

2.2.4 *Column adsorption experiments*

Continuous adsorption experiments in fixed-bed column were conducted in a glass column (1.1-cm inner diameter and 37.5 cm length), provided with Teflon stopper. All experiments were performed by gravity elution. A coffee filter followed by a bed of cotton was placed at the end of the column to avoid blockage. The pecan packing material (0.05 ± 0.0005 g) was carefully added. In order to avoid void volumes and air gaps, the column was shaken during the packing, and after packing, another cotton bed was placed to apply pressure. The breakthrough experiments were performed for each of the two PNH varieties (Barton and Native). The experiments were performed at two different pH values (2.5 ± 0.02 and 6.18 ± 0.1) of the influent solution and at two particle sizes (0.42 mm and 0.85 mm). The influent solution of 2.28 ± 0.1 mg/L Cr(VI) was passed to a constant flow rate of 1.54 mL/min adjusting the stopcock opening. Effluent samples were collected every minute for the first 5 min after this time, samples were collected each 5 min until the Cr (VI) concentration of the effluent became equal the feed concentration or until not changes on the Cr (VI) concentration of the effluent were observed. The Cr(VI) and total Cr concentration in the effluent was determined using a UV/VIS and atomic absorption spectrometry, respectively as previously described. The experiments were conducted in triplicate at room temperature (27 ± 0.85ºC).

Data of Cr concentrations versus time were used to construct the breakthrough curves. The breakthrough curve graphically describes the performance of the fixed-bed column and allow us to obtain the operation and dynamic responses of an adsorption column (Han *et al*., 2009). These were obtained by plotting C_t/C_0 with respect to time for a given bed depth, where C_t and C_0 are the effluent and influent concentrations, respectively (Chen *et al*., 2012). The time required for the effluent concentration to reach a specific breakthrough concentration is known as breakthrough time (Mondal, 2009). The 50% breakthrough time is established when the metal concentration in the effluent reaches 50% of the inlet concentration. Also, parameters like the concentration at equilibrium, removal rate, and exhaust time were obtained from the breakthrough curves. The concentration in equilibrium (mg/L) was considered when the breakthrough curve showed an asymptotic behavior, it was selected when there was no statistical difference in the effluent concentration of Cr(VI); and at this point was chosen the exhaust time (min). The removal rate (mg/L min) was calculated as the slope of the linear section in the breakthrough curves.

2.2.5 *Modeling of adsorption data*

The modelling data of the breakthrough curves were analysed using the Thomas model. This model assumes that the rate driving force obeys second-order reversible reaction kinetics, the Langmuir kinetics of adsorption-desorption, and no axial dispersion. The Thomas model is given as follows Eq (1) (Shahbazi *et al*., 2011):

$$\frac{C_t}{C_0} = \frac{1}{1 + \exp((K_(Th)q_(Th)m/Q) - K_(Th)C_0t)} \quad (1)$$

where C_t is the effluent concentration (mg/L), C_0 is the influent concentration (mg/L), K_{Th} is the Thomas rate constant (mL/min mg), q_{Th} is the Thomas maximum adsorption capacity of the adsorbent (mg/g), m is the mass of the adsorbent (g), Q is the flow rate (mL/min), and t is the time (min).

The experimental data of C_t/C_0 against t were plotted to obtain the kinetics parameter constants (K_{Th} and q_{Th}). The data were fitted with the Thomas model to obtain the kinetic coefficient K_{Th} and the adsorption capacity of the column q_{Th} for each condition using the non-linear regression method.

2.2.6 *Statistical analysis*

A $2 \times 2 \times 2$ completely randomized factorial design was used. The adsorption experiments were performed in triplicate, and the values reported are the mean

plus or minus the standard deviation to determine the influence of the PNH variety (Barton and Native), pH solution (2.5 ± 0.02 and 6.18 ± 0.12), and particle size (0.42 mm and 0.85 mm) on the removal of Cr(VI) in the effluent solution. Analysis of variance and means difference were performed using the Tukey test with a significance level of 5% using Minitab version 17.1 software (Minitab 17.1, 2013). Likewise, the experimental data was adjusted from the Thomas model using non-linear regression to obtain q_{Th} and K_{Th} (Eq 1). The quality of the fit between the experimental data and predicted theoretical values was evaluated by determination coefficients (R^2). The fitted model was performed using SAS software version 9.2 (SAS 9.2, 2007) (Cary, NC, USA) at a confidence level of 95%.

3 Results and discussion

Table 1 shows the chemical characteristics of Barton and Native PNHs. Native PNHs present higher fiber content than Barton PNHs, and this is directly related to different varieties of pecan as each has their own special and unique characteristics. Barton PNHs had a higher tannin content than Native PNHs, as well as higher total polyphenols, which was attributed to the variety of pecan nut husk (Pinheiro do Prado *et al*., 2013). In a previous study with pericarp of *Carya illinoinensis* (Hernández-Montoya *et al*., 2011), the content of ash reported (1.7%) was lower than that obtained in our study (11.61 and 10.38% for Barton and Native PNH, respectively). This difference can be attributed to the removal of the dark brown layers during the washing step. The pHpzc values of 4.98 and 5.64 were obtained for Barton and Native PNHs, respectively; these values are close to the value of 5.2 reported for pecan pericarp (Hernández-Montoya *et al*., 2011). The difference between the pH_{pzc} values of Barton and Native husks can be attributed to the difference in concentration of the surface functional groups. From these results, the Native PNH can be inferred to have slightly more positively charged functional groups.

3.1 Thermal properties

The thermogravimetric analysis of PNHs shows the thermal decomposition processes associated with this lignocellulosic material. The thermogravimetric analysis (TGA) and differential thermal analysis (DTA) curves for both PNH varieties (Figure 1) are similar, and the thermic events observed are commonly assigned to water loss and to the degradation of hemicellulose, cellulose, and lignin (Yang *et al*., 2007). The pattern of TGA curves for both PNHs is similar to the reported pattern for the pericarp of pecan (Hernández-Montoya *et al*., 2011). Both TGA curves show that an initial mass loss due to evaporation of moisture occurs below 100°C, and some overlapping peaks are observed.

Table 1. Chemical properties of pecan nut husks.

Parameter	PNH Variety	
	Barton*	Native*
Moisture (%)	6.28 ± 0.05	6.94 ± 0.03
Ash (%)	11.61 ± 0.12	10.38 ± 0.05
Lipids (%)	5.36 ± 0.5	5.26 ± 0.14
Protein (%)	6.34 ± 0.1	6.18 ± 0.1
Fiber (%)	18.77 ± 0.7	30.58 ± 0.3
Carbohydrates (%)	51.66 ± 0.3	40.66 ± 0.2
Tannins (%)	11.56 ± 0.2	3.17 ± 0.003
Total polyphenols (mg EAG/100g)	1563 ± 7.2	270.6 ± 1.5

* Mean ± standard deviation

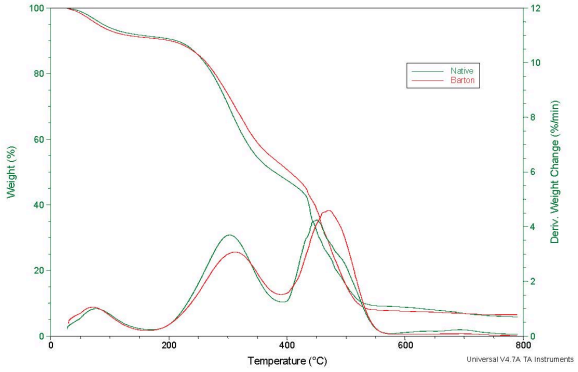

Fig. 1. Thermogravimetric and differential thermal analysis curves of Barton and Native pecan nut husks.

The mass loss observed from approximately 150 to 500°C is due to hemicellulose, cellulose, and lignin, which are the main components of lignocellulosic materials (Yang *et al*., 2007), and they usually appear as two peaks (Garcia-Perez *et al*., 2001). These components are thermochemically decomposed in the range of 150 to 350, 275 to 350, and 250 to 500°C for hemicellulose, cellulose, and lignin, respectively (Hernández-Montoya *et al*., 2011). The complex composition of lignocellulosic materials, as well as the number reactions during the pyrolysis process, make difficult to accurately determine the composition of this material (Elizalde-Gonzalez and Hernandéz-Montoya, 2007).

3.2 FTIR analysis

The ATR-FTIR spectra indicate the presence of functional groups in both PNHs (Figures 2 and 3). Barton and Native PNHs have similar ATR-FTIR spectral results. Both FTIR spectra are in good agreement with a previous study on the pericarp of *Carya illinoinensis* (Hernández-Montoya *et al*., 2011). Because PNHs are a complex lignocellulosic material, the ATR-FTIR spectrum displays different bands. The broad band around 3600-2900 cm^{-1} indicates the O-H bond (hydroxyl group), with a maximum at 3306 and 3303 cm^{-1} for Barton and Native PNHs, respectively. In this same range, the overlapping of the N-H bond occurs; however, the peaks in the frequency 1019 and 1029 cm^{-1} for Native and Barton PNHs, respectively, indicate the presence of the aliphatic amine functional group. The two peaks (2926 and 2853 cm^{-1}) for Barton PNHs and (2919 and 2851 cm^{-1}) for Native PHNs correspond to the aliphatic bond C-H, and this bond will also vibrate at 1436 and 1435 cm^{-1}.

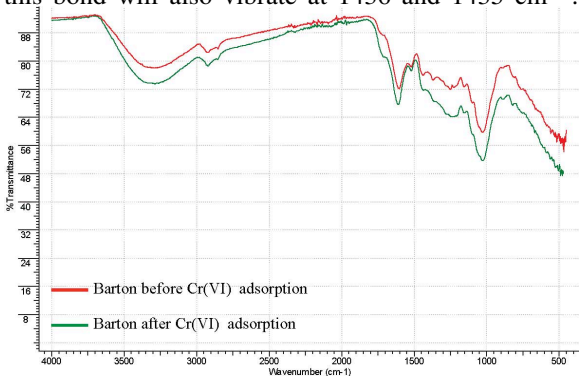

Fig. 2. The FTIR spectra of Barton PNHs before and after Cr(VI) adsorption.

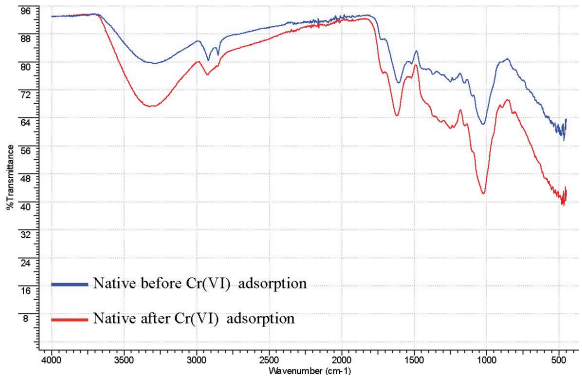

Fig. 3. The FTIR spectra of Native PNHs before and after Cr(VI) adsorption.

Carbonyl bands are observed at 1716 and 1731 cm^{-1} for Barton and Native PNHs, respectively. Peaks at 1603 and 1606 cm^{-1} are assigned to the C=C bond of aromatic rings. The peaks at 1029 and 1030 cm-1 might represent the C-O bond of either an ether or ester group (Aguayo-Villareal *et al*., 2013). All chemical groups found in the ATR-FTIR spectra form parts of the cellulose, hemicellulose, lignin, polyphenol, and tannin structures. These structures all have the groups OH, C=O, C-O-C, aromatic rings, and C-H bonds in common; these same vibrations were also reported for pure oak tannins, and they were associated with ellagic acid, which is the main constituent of oak tannins (Puică *et al*., 2006). Figures 2 and 3 show the possible interaction of the functional groups present in both PNH varieties with Cr(VI). The bands of the spectra corresponding to the PNHs with adsorbed Cr(VI) are slightly broader than the PNHs alone, suggesting the formation of chromium complexes on the surface of the material (Hon and Chang, 1985).

Table 2. Semi quantitative EDX analysis (%wt.) of Barton PNH with a 0.42 mm particle size before and after Cr(VI) adsorption.

	Elements			
Treatment	C	O	K	Cr
Before	64.06	34.44	1.49	Nd
After	64.79	34.53	0.54	0.14

Nd.- not detected

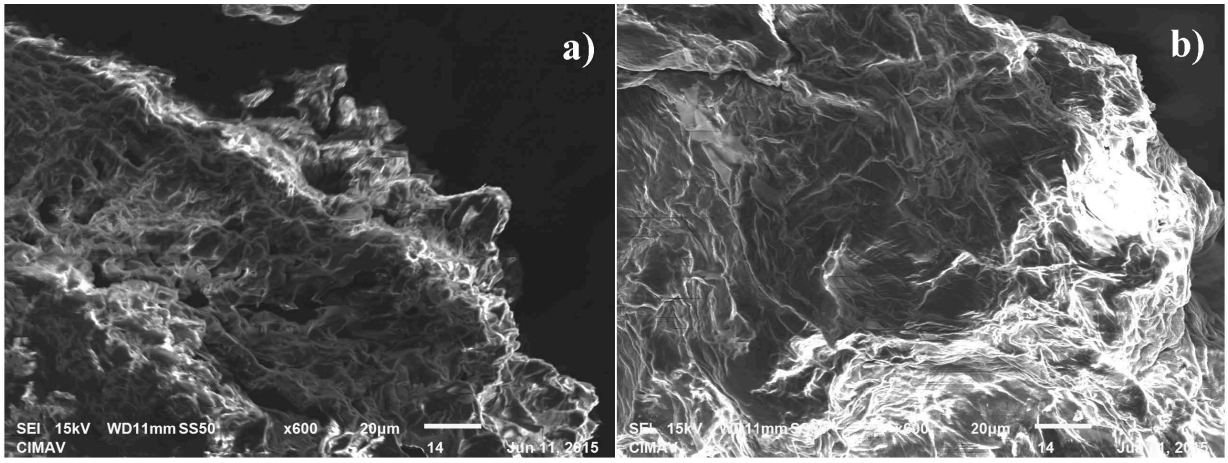

Fig. 4. The SEM micrographs of Barton PNH with a 0.42-mm particle size (a) before and (b) after Cr(VI) adsorption.

The carboxyl (1716 and 1731 cm^{-1}) and hydroxyl (3306 and 3303 cm^{-1}) groups, which are apparently involved in the adsorption process, show a decrease in intensity after metal binding (Elangovan *et al*., 2008b; Chen *et al*., 2011).

3.3 Barton PNH SEM analysis

Scanning electron micrographs of Barton PNHs before and after Cr(VI) adsorption are shown in Figure 4. Before Cr(VI) adsorption, some pores are observed. However, after Cr(VI) adsorption, no pores are observed, showing a smoother surface; this is due to the adsorption of Cr(VI) on the surface (Malkoc *et al*., 2006). Table 2 presents the EDX analysis, showing the presence of C, O, and K. After the exposure to Cr(VI), the adsorption of Cr(VI) onto the surface of Barton PNH is evident.

3.4 Breakthrough curves

The breakthrough curves at pH of 2.5 ± 0.02 for Barton and Native PNHs with particle size of 0.85 and 0.42 mm are shown in Figure 5. In all breakthrough curves, the reduction to Cr(III) and adsorption of Cr(VI) are observed. The breakthrough curves further show when Cr(III) appears in the eluent, which was not present in the influent solution. The chemical reduction of Cr(VI) is very fast due to its high redox potential (Elangovan *et al*., 2008b). The reduction to Cr(III) is produced and favored for both PNH varieties at an acid pH (2.5) in the presence of phenols and tannins (Elangovan *et al*., 2008b), which promote the reduction in both PNH varieties. This reduction has also been observed for different biomaterials such as palm flowers (Elangovan *et al*., 2008a) and aquatic weeds (Elangovan *et al*., 2008b). The concentration of polyphenols and tannins is higher in Barton PNHs; hence, its Cr(III) concentration in the effluent is higher than that in the Native effluent. The advantage of the chemical reduction is that Cr(III) is less toxic, less soluble, and also less mobile in the environment (Barrera-Díaz *et al*., 2012; McLean *et al*., 2012), but the release of organic compounds in the effluent increases the oxygen demand in water. From the curves, the concentration of Cr(VI) decreases as the concentration of Cr(III) increases; this same behavior was also reported for banana skin (Park *et al*., 2008).

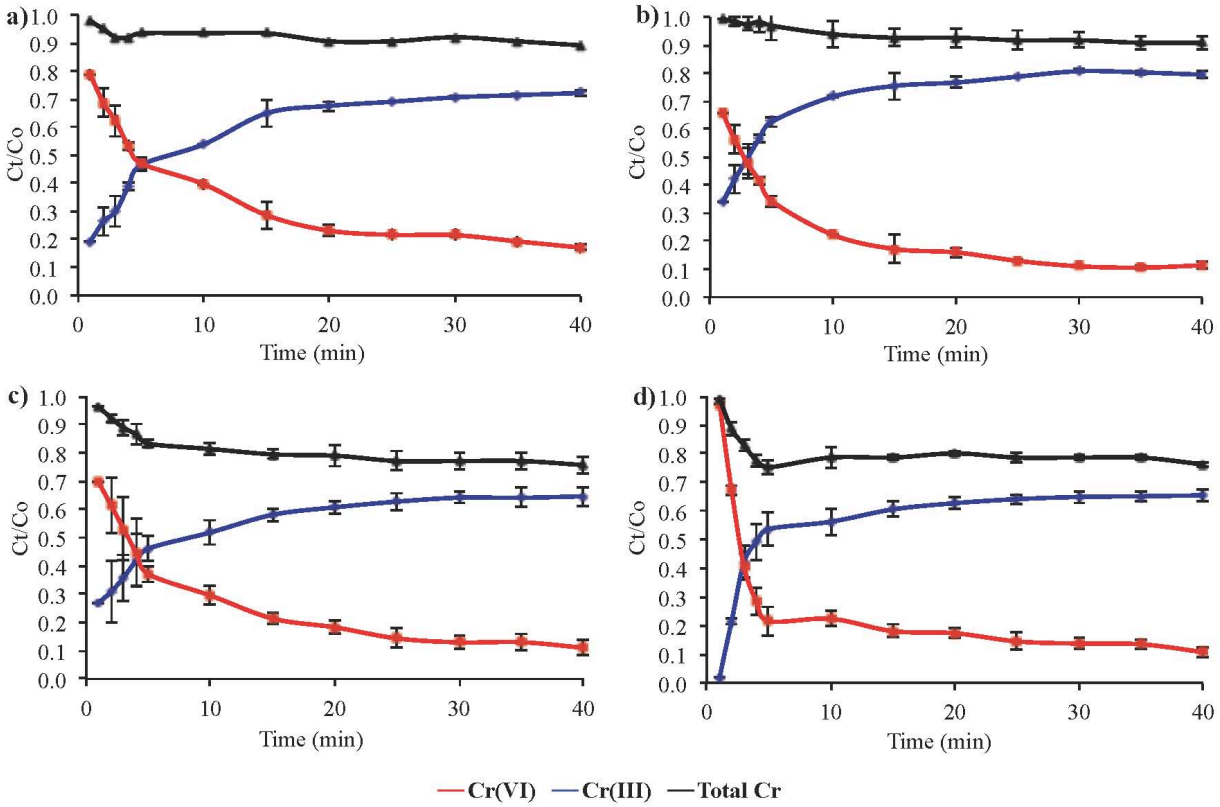

Fig. 5. Breakthrough curves for chromium species at pH 2.5 ± 0.02 for (a,c) Barton and (b,d) Native PNH varieties with two particle sizes: Barton PNHs with particle sizes of (a) 0.85 mm and (c) 0.42 mm, and Native PNHs with particle sizes of (b) 0.85 mm and (d) 0.42 mm at an influent chromium concentration of 2.28 ± 0.1 mg/L, PNH mass of 0.05 ± 0.0005 g, and flow rate 1.54 mL/min.

The concentration of total Cr is also shown, and the time required to reach equilibrium of the Cr species is around 12 min for all conditions. Besides the chemical reduction of Cr(VI), adsorption of Cr(VI) is observed. The largest 50% breakthrough time (8.5 min) was for Barton PNHs with a 0.42-mm particle size. The 50% breakthrough time increases as the particle size decreases; for Barton PNH particle sizes of 0.85 and 0.45 mm, the 50% breakthrough times were 5 min and 8.5 min, respectively. On the other hand, the 50% breakthrough time for Native PNH particle sizes of 0.85 mm and 0.45 mm were 3 min and 4 min, respectively. This could be attributed to the larger surface area in smaller particle size (Zheng *et al.*, 2010).

The breakthrough curves at a pH of 6.18 ± 0.1 for Barton and Native PNHs with particle sizes of 0.85 and 0.42 mm are shown in Figure 6. For all breakthrough curves, only a fraction of the inlet Cr(VI) solution was adsorbed by the Native and Barton husks, and the remaining fraction was present in the effluent solution as Cr(III) (Elangovan *et al.*, 2008a) due to chemical reduction to Cr(III) and adsorption of Cr(VI). The reduction to Cr(III) is produced for both PNH varieties at a pH of 6.18 due to the phenol and tannin contents (Table 1) (Elangovan *et al.*, 2008b). Similar to that for pH 2.5, the concentration of Cr(VI) decreases when the concentration of Cr(III) increases. Moreover, the Cr total concentration is shown to reach equilibrium of the Cr species in 30 min for Barton PNHs and 15 min for Native PNHs. For the adsorption of Cr(VI), Barton PNHs with particle size of 0.85 mm showed the largest 50% breakthrough time (14 min). The 50% breakthrough time increased as the particle size increased. For Barton PNH particle sizes of 0.85 mm and 0.45 mm, the 50% breakthrough times were 14 min and 12 min, respectively. On the other hand, the 50% breakthrough time for Native PNH particle sizes of 0.85 mm and 0.45mm were 4.5 min and 3.5 min, respectively. This is could be attributed to the fact that Cr(VI) anions are not able to penetrate into the pores of large particle sizes (Gupta *et al.*, 2010).

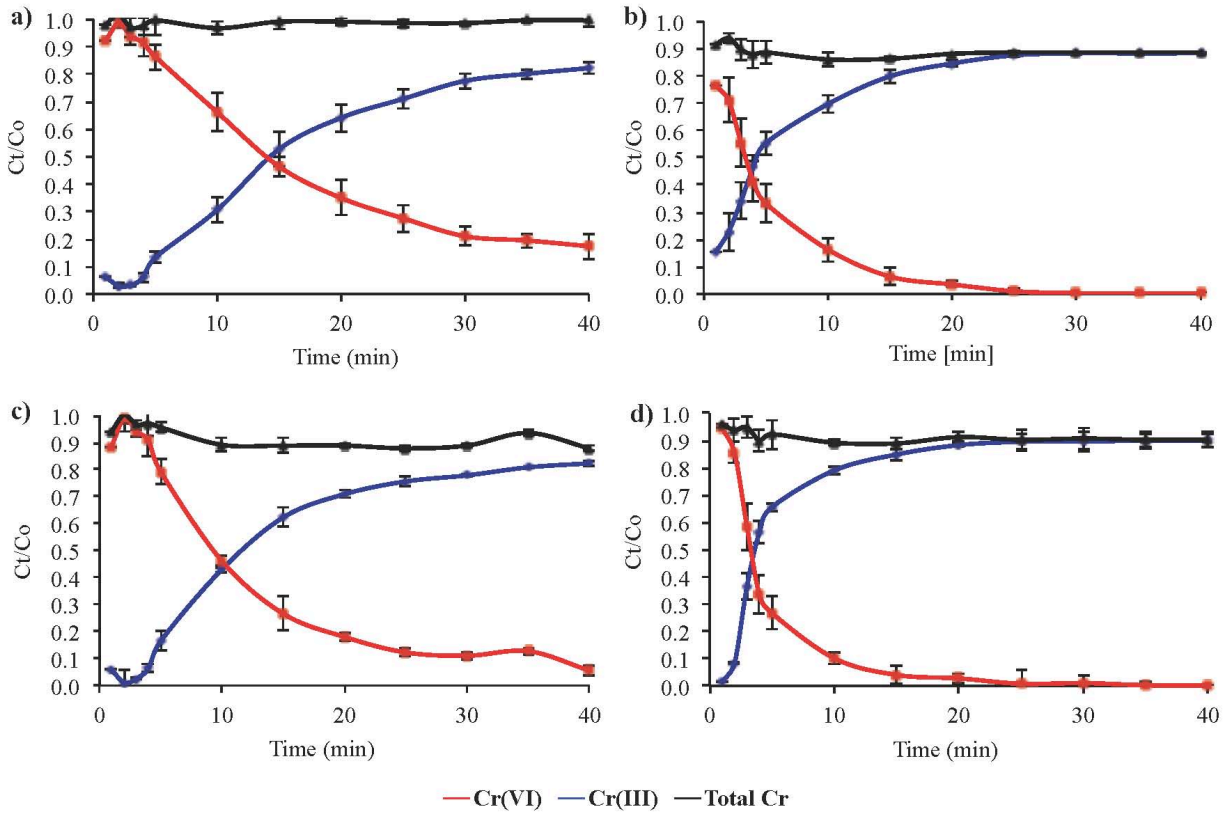

Fig. 6. Breakthrough curves for chromium species at pH 6.18 ± 0.1 for (a,c) Barton and (b,d) Native PNHs with two particle sizes: Barton PNHs with particle sizes of (a) 0.85 mm and (c) 0.42 mm, and Native PNHs with particle sizes of (b) 0.85 mm and (d) 0.42 mm at an inlet chromium concentration of 2.28 ± 0.1 mg/L, PNH mass of 0.05 ± 0.0005 g, and flow rate of 1.54 mL/min.

When absorption conditions are compared at different pH values (Figures 5 and 6), a shift from the right to left is observed in the breakthrough curves for Barton PNH at pH 2.5, suggesting that less Cr(VI) was removed. Barton PNH at an acidic pH would require less time to reach equilibrium; therefore, it has better Cr(VI) removal performance.

3.5 Concentration in equilibrium

The concentration at equilibrium (mg/L), removal rate (mg/L min), and exhaust time (min) were obtained from the breakthrough curves. These parameters are important for indicating the packing material performance in the column in the removal of metals. The concentration of Cr(VI) in equilibrium was selected as the time where the concentration in the effluent presented asymptotic behavior; when there were no significant differences in its concentration. The concentration of Cr(VI) at equilibrium was affected significantly (p <0.05) by the PNH variety, PNH particle size, and pH of the influent solution, and their interactions (Table 3).

Table 3 shows that a lower Cr(VI) concentration was achieved in equilibrium with small PNH particle sizes (0.42 mm) because small particles sizes lead to an increased surface area (Zheng *et al.*, 2010). Hence, there are more sites available for solute-surface interaction (Gupta *et al.*, 2010; Maleki *et al.*, 2011). However, for both particle sizes, the maximum concentration of Cr(VI) in the effluent was reached with Native PNHs at a pH of 6.18; its saturation almost equaled the influent Cr(VI) concentration. For both PNH varieties, there is a tendency for the concentration in equilibrium at a pH of 6.18 to increase; this is possibly due to the abundance of negatively charged hydroxyl ions that cause hindrance between the Cr(VI) anions and the surface of the material (Gupta *et al.*, 2010). For both PNH varieties, the lowest Cr(VI) concentrations occurred with the smallest particle sizes (0.42 mm) and the lowest pH (2.5), meaning that the adsorbent is capable of

adsorbing more of the metal. However, the Cr(VI) adsorption will be very slow because these conditions require a long time to reach saturation.

The pH of the influent solution is an important parameter to consider during the metal uptake process. The metal chemical reduction and adsorption on the surface of the biomaterial are attributed to the pH of the solution (Gupta and Babu, 2009) due to changes in the metal oxidation states (Yipmantin *et al*., 2011) and alteration of the reactive surface groups by protonation or deprotonation of the biomaterial. At an acidic pH (2.5), the oxo-anions H_2CrO_4, CrO_4^{2-}, and $Cr_2O_7^{2-}$ are reduced to Cr(III) (Gupta *et al*., 2010); thus, the concentration of Cr(VI) in the effluent was the lowest. Moreover, the pH of the influent solution affects the charge of the surface functional groups of the adsorbent by acquiring negative or positive charges. The pH at the point zero charge (pH_{pzc}) of the adsorbent gives information about the charge of the surface functional groups, indicating the pH at which the amount of positive and negative charges on the adsorbent surface is equal (Chen *et al*., 2011). The pH_{pzc} values of Barton (4.98) and Native (5.64) PNHs, indicate that Barton PNHs have more positively charged functional groups. This larger number of positively charged functional groups could be due to the polyphenol and tannin contents, which are higher in Barton PNHs than in Native PNHs (Table 1). Below the pH_{pzc} of PNH, the surface charge of both PNHs is positive. Therefore, at a pH value of 2.5, an electrostatic attraction probably occurs between anionic Cr(VI) and positive surface of both PNH varieties, lowering the concentration of Cr(VI) in the effluent. On the other hand, when the pH is above pH_{pzc}, the PNH surface became more negative, and the electrostatic repulsion between the anionic form of Cr(VI) and the PNH surface sites increases, resulting in a high concentration of Cr(VI) in the effluent (Ozdes *et al*., 2014).

The removal rate was significant affected (p <0.05) by the PNH variety. The fastest removal rate corresponded to Native PNHs with a particle size of 0.42 mm for both considered pH values. On the other hand, the slowest removal rate was for Barton PNHs, regardless of the particle size and pH value. Native pecans present a hard and thick pericarp, compared to that of the Barton variety. This result can probably be attributed to the chemical composition of Native pecans, where the lignin content is likely higher. The exhaustion time, which corresponds to the time where the breakthrough curve reaches a plateau, was selected when there was no statistical difference in the effluent concentration of Cr(VI). The values for the exhaustion time ranged from 10 to 30 min. Both sizes of Barton PNHs at pH 6.18 presented the largest exhaustion times in comparison with Native PNHs, for which the influence of the low pH of the influent solution was observed to decrease the exhaustion time. This result suggests that the polyphenol and tannin content of the Barton PNH, which were between 3 and 5 times higher that of Native PNHs (Table 1), could favor Cr(VI) adsorption, which was evident at the lowest pH (2.5).

Table 3. Concentration in equilibrium[1], removal rate[1], and exhaustion time for Barton and Native PNHs for the removal of Cr(VI) using different particle sizes and pH.

PNH	Particle size (mm)	pH	Concentration in equilibrium mg/L	Removal rate mg/L·min	Exhaustion time (min)
Barton	0.42	2.5 ± 0.02	1.235 ± 0.057^{e}	0.028 ± 0.001^{c}	10
	0.85		1.546 ± 0.043^{d}	0.031 ± 0.001^{c}	15
	0.42	6.18±0.1	1.853 ± 0.01^{b}	0.030 ± 0.001^{c}	30
	0.85		1.848 ± 0.042^{bc}	0.029 ± 0.000^{c}	30
Native	0.42	2.5 ± 0.02	1.339 ± 0.062^{e}	0.052 ± 0.001^{a}	10
	0.85		1.706 ± 0.0987^{c}	0.039 ± 0.004^{bc}	10
	0.42	6.18±0.1	2.021 ± 0.0134^{a}	0.056 ± 0.002^{a}	15
	0.85		1.903 ± 0.026^{ab}	0.044 ± 0.004^{ab}	15

* Mean ± standard deviation. Values with different letters by the column indicate significant differences (p <0.05), Tukey's test.

Table 4. Kinetic constants for Thomas Model.

Variety	Particle size (mm)	pH	K_{Th} mL/min.mg	q_{Th} mg/g	R^2
Barton	0.42	2.5 ± 0.02	0.0254 ± 0.0083^{c}	769.5 ± 78.4^{a}	0.79
	0.85		0.0382 ± 0.0006^{c}	633.45 ± 2.47^{b}	0.80
	0.42	6.18±0.1	0.0981 ± 0.0031^{b}	709.2 ± 2.83^{ab}	0.89
	0.85		0.0862 ±0.0015^{b}	791.35 ± 2.9^{a}	0.94
Native	0.42	2.5 ± 0.02	0.0296 ± 0.0001^{c}	750 ± 15^{a}	0.55
	0.85		0.0389 ± 0.0006^{c}	44.15 ± 2.74^{e}	0.73
	0.42	6.18±0.1	0.5488 ± 0.007^{a}	180.75 ± 6.43^{d}	0.87
	0.85		0.1031 ± 0.019^{b}	317.85 ± 6.72^{c}	0.90

[1] Mean ± standard deviation. Values with different letter by column indicates significant difference (p <0.05), Tukey´s test. K_{Th} = Rate constant; q_{Th} = the equilibrium maximum adsorption capacity; R^2 = Determination coefficient.

3.6 Thomas model

Data from the fixed-bed adsorption columns were fitted to the Thomas model in order to determine the rate constant (K_{Th}) and the equilibrium maximum adsorption capacity (q_{Th}) of Cr(VI). The Thomas model constants are shown in Table 4. The Thomas model adequately represented the relationships with satisfactory R^2 values, except for some experimental conditions of Native PNHs, which presented the lowest R^2 values. The K_{Th} values range from 0.5488 to 0.0254 mL/min mg. The highest value occurred for Native PNH with a 0.42-mm particle size at a pH of 6.18, and the lowest value occurred for Barton PNH with a 0.42-mm particle size at a pH of 2.5. The q_{Th} values range between 791.35 and 180.75 mg/g. The q_{Th} value for both PNHs at a pH of 2.5 show higher values for the smallest particle size (0.42 mm), while a contrary behavior is observed at pH 6.18. The best fitting was obtained for Barton PNHs with a 0.85-mm particle size at a pH of 6.18, and the lowest fitting correspond to Native PNHs with a particle size of 0.42 mm at a pH of 2.5. In general, the Thomas model is capable of describing the adsorption process for the majority of the experimental conditions (Chen *et al.*, 2012). However, the model could satisfactorily predict the adsorption process (high values of R^2) for Barton PNHs due to its kinetic behavior (Figures 5 and 6), which has slower removal rates than Native PNHs

(Table 4); this is perhaps related to the adsorption capacity for high polyphenol and tannin contents.

Conclusions

The chemical reduction of Cr(VI) to Cr(III) and adsorption of Cr(VI) were performed satisfactorily in a fixed-bed column using Barton and Native pecan nut husks as the packing material. Native PNHs had a higher concentration in equilibrium and a shorter exhaustion time in the column. On the other hand, the Barton PNHs showed better characteristics for the adsorption of Cr(VI) and Cr(III), showing longer exhaustion times at higher pH values and concentrations in equilibrium similar to that of Native PNH. The characteristics presented by Barton PNHs were related to the high tannin and phenolic compound contents. The FT-IR spectra reveled the functional groups involved in the adsorption of Cr(VI). The SEM with EDX detector shows the presence of chromium in the PNH after chromium adsorption. Moreover, the Thomas model was adequately fitted to the experimental data from the breakthrough curves, showing satisfactory fitting for Barton PNH (R2 of 0.79-0.94) with a higher capacity of adsorption (q_{Th}) than that of Native PNHs. The results obtained suggest that Barton PNHs could be used as an inexpensive alternative packing material for removing Cr(VI) from groundwater and waste water.

Acknowledgements

The authors acknowledge FCQ-UACH through Secretaría de Investigación and to PRODEP for a scholarship to M.C.C.E. This work was partially supported by FCQ-UACH and PRODEP.

Nomenclature

C_t	effluent concentration, mg/L
C_0	influent concentration, mg/L
K_{Th}	Thomas rate constant, mL/min mg
q_{Th}	Thomas maximum adsorption capacity of the adsorbent, mg/g
m	mass of the adsorbent, g
Q	flow rate, mL/min
t	time, min

References

Aguayo-Villarreal, I.A., Ramírez-Montoya, L.A., Hernández-Montoya, V., Bonilla-Petriciolet, A., Montes-Morán, M.A., Ramírez-López, E.M. (2013). Sorption mechanism of anionic dyes on pecan nut shells (*Carya illinoinensis*) using batch and continuous systems. *Industrial Crops and Products 48*, 89-97. DOI: 10.1016/j.indcrop.2013.04.009

Aliabadi, M., Morshedzadeh, K., Soheyli, H. (2006). Removal of hexavalent chromium from aqueous solution by lignocellulosic solid wastes. *International Journal of Environmental Science and Technology 3*, 321-325. DOI: 1007/BF03325940

AOAC International. (1998). *Official Methods of Analysis* (16th ed). AOAC. Arlington, VA, USA.

APHA. (1975). *Standard Methods for Examination of Water and Wastewater* (14th ed.). American Public Health Association, Pp 192-194 .Washington, DC, USA.

Badillo-Camacho, J., Murillo-Delgado, J. O., Barcelo-Quintal, I. D., del Valle, P. Z., Orozco-Guareño, E., López-Chuken, U. J., Gomez-Salazar, S. (2016). Heavy metals speciation in sediments of a Mexican tropical lake. *Revista Mexicana de Ingeniería Química 15*, 565-573.

Bansal, M., Garg, U., Singh, D., Garg, V.K. (2009). Removal of Cr (VI) from aqueous solutions using pre-consumer processing agricultural waste: A case study of rice husk. *Journal of Hazardous Materials 162*, 312-320. DOI: 10.1016/j.jhazmat.2008.05.037

Barrera-Díaz, C.E., Lugo-Lugo, V., Bilyeu, B.A. (2012). Review of chemical, electrochemical and biological methods for aqueous Cr (VI) reduction. *Journal of Hazardous Materials 223*, 1-12. DOI: 10.1016/j.jhazmat.2012.04.054

Bhattacharya, A.K., Naiya, T.K., Mandal, S.N., Das, S.K. (2008). Adsorption, kinetics and equilibrium studies on removal of Cr(VI) from aqueous solutions using different low-cost adsorbents. *Chemical Engineering Journal 137*, 529-541. DOI: 10.1016/j.cej.2007.05.021

Bielicka, A., Bojanowska, I., Wisniewski, A. (2005). Two faces of chromium-pollutant and bioelement. *Polish Journal of Environmental Studies 14*, 5-10.

Chen, S., Yue, Q., Gao, B., Li, Q., Xu, X. (2011). Removal of Cr (VI) from aqueous solution using modified corn stalks: Characteristic, equilibrium, kinetic and thermodynamic study. *Chemical Engineering Journal 168*, 909-917. DOI: 10.1016/j.cej.2011.01.063

Chen, S., Yue, Q., Gao, B., Li, Q., Xu, X., Fu, K. (2012). Adsorption of hexavalent chromium from aqueous solution by modified corn stalk: A fixed-bed column study. *Bioresource Technology 113*, 114-120. DOI: 10.1016/j.biortech.2011.11.110

Chowdhury, Z.Z., Hamid, S.B.A., Das, R., Hasan, M.R., Zain, S.M., Khalid, K., Uddin, M.N. (2013). Preparation of carbonaceous adsorbents from lignocellulosic biomass and their use in removal of contaminants from aqueous solution. *BioResources 8*, 6523-6555.

Chu, K. H. (2004). Improved fixed bed models for metal biosorption. *Chemical Engineering Journal 97*, 233-239. DOI: 10.1016/S1385-8947(03)00214-6

Demirbas, A. (2008). Heavy metal adsorption onto agro-based waste materials: A review. *Journal of Hazardous Materials 157*, 220-229. DOI: 10.1016/j.jhazmat.2008.01.024

Dhal, B., Thatoi, H.N., Das, N.N., Pandey, B.D. (2013). Chemical and microbial remediation of hexavalent chromium from contaminated soil and mining/metallurgical solid waste: a review. *Journal of Hazardous Materials 250*, 272-291. DOI: 10.1016/j.jhazmat.2013.01.048

Elangovan, R., Philip, L., Chandraraj, K. (2008a). Biosorption of hexavalent and trivalent chromium by palm flower (*Borassus aethiopum*). *Chemical Engineering Journal 141*, 99-111. DOI: 10.1016/j.cej.2007.10.026

Elangovan, R., Philip, L., Chandraraj, K. (2008b). Biosorption of chromium species by aquatic weeds: Kinetics and mechanism studies. *Journal of Hazardous Materials 152*, 100-112. DOI: 10.1016/j.jhazmat.2007.06.067

Elizalde-González, M.P., Hernández-Montoya, V. (2007). Characterization of mango pit as raw material in the preparation of activated carbon for wastewater treatment. *Biochemical Engineering Journal 36*, 230-238. DOI: 10.1016/j.bej.2007.02.025

El-Sheikh, A.H., Hilal, M.M. A., Sweileh, J.A. (2011). Bio-separation, speciation and determination of chromium in water using partially pyrolyzed olive pomace sorbent. *Bioresource Technology 102*, 5749-5756. DOI: 10.1016/j.biortech.2011.03.021

Farooq, U., Kozinski, J.A., Khan, M.A., Athar, M. (2010). Biosorption of heavy metal ions using wheat based biosorbents-A review of the recent literature. *Bioresource Technology 101*, 5043-5053. DOI: 10.1016/j.biortech.2010.02.030

Gadd, G.M. (2009). Biosorption: Critical review of scientific rationale, environmental importance and significance for pollution treatment. *Journal of Chemical Technology and Biotechnology 84*, 13-28. DOI: 10.1002/jctb.1999

García-Perez, M., Chaala, A., Yang, J., Roy, C. (2001). Co-pyrolysis of sugarcane bagasse with petroleum residue. Part I: Thermogravimetric analysis. *Fuel 80*, 1245-1258. DOI: 10.1016/S0016-2361(00)00215-5

Gardea-Torresdey, J.L., De la Rosa, G., Peralta-Videa, J.R. (2004). Use of phytofiltration technologies in the removal of heavy metals: A review. *Pure and Applied Chemistry 76*, 801-813. DOI: 10.1351/pac200476040801

Gautam, R.K., Mudhoo, A., Lofrano, G., Chattopadhyaya, M.C. (2014). Biomass-derived biosorbents for metal ions sequestration: Adsorbent modification and activation methods and adsorbent regeneration. *Journal of Environmental Chemical Engineering 2*, 239-259. DOI: 10.1016/j.jece.2013.12.019

Gupta, S., Babu, B.V. (2009). Modeling, simulation, and experimental validation for continuous Cr (VI) removal from aqueous solutions using sawdust as an adsorbent. *Bioresource Technology 100*, 5633-5640. DOI: 10.1016/j.biortech.2009.06.025

Gupta, V.K., Rastogi, A., Nayak, A. (2010). Adsorption studies on the removal of hexavalent

chromium from aqueous solution using a low cost fertilizer industry waste material. *Journal of Colloid and Interface Science 342*, 135-141. DOI: 10.1016/j.jcis.2009.09.065

Hadjigeorgalis, E., Lilllywhite, J.M., Herrera, E. International Trade in Pecans. Available online: http://aces.nmsu.edu/pubs/_z/Z503/welcome.html. Accessed on 01 May 2015.

Han, R., Wang, Y., Zhao, X., Wang, Y., Xie, F., Cheng, J., Tang, M. (2009). Adsorption of methylene blue by phoenix tree leaf powder in a fixed-bed column: Experiments and prediction of breakthrough curves. *Desalination 245*, 284-297. DOI: 10.1016/j.desal.2008.07.013

Hernández-Montoya, V., Mendoza-Castillo, D.I., Bonilla-Petriciolet, A., Montes-Morán, M.A., Pérez-Cruz, M.A. (2011). Role of the pericarp of *Carya illinoinensis* as biosorbent and as precursor of activated carbon for the removal of lead and acid blue 25 in aqueous solutions. *Journal of Analytical and Applied Pyrolysis 92*, 143-151. DOI: 10.1016/j.jaap.2011.05.008

Hon, D.N.S., Chang, S.T. (1985). Photoprotection of wood surfaces by wood-ion complexes. *Wood and Fiber Science 17*, 92-100.

Khan, N.A., Ibrahim, S., Subramaniam, P. (2004). Elimination of heavy metals from wastewater using agricultural wastes as adsorbents. *Malaysian Journal of Science 23*, 43-51.

Kosmulski, M. (2004). pH-dependent surface charging and points of zero charge II. Update. *Journal of Colloid and Interface Science 275*, 214-224. DOI: 10.1016/jcis.2004.02.029

Kyzas, G.Z., Kostoglou, M. (2014). Green adsorbents for wastewaters: A critical review. *Materials 7*, 333-364. DOI: 10.3390/ma7010333

Li, W., Gong, X., Li, X., Zhang, D., Gong, H. (2012). Removal of Cr (VI) from low-temperature micro-polluted surface water by tannic acid immobilized powdered activated carbon. *Bioresource Technology 113*, 106-113. DOI: 10.1016/j.biortech.2011.12.037

Maleki, A., Mahvi, A.H., Zazouli, M.A., Izanloo, H., Barati, A.H. (2011). Aqueous cadmium removal by adsorption on barley hull and barley hull ash. *Asian Journal of Chemistry 23*, 1373-1376.

Malkoc, E., Nuhoglu, Y., Dundar, M. (2006). Adsorption of Cr C(VI) on pomace-An olive oil industry waste: Batch and column studies. *Journal of Hazardous Materials 138*, 142-151. DOI: 10.1016/j.jhazmat.2006.05.051

McLean, J.E., McNeill, L.S., Edwards, M., Parks, J.L. (2012). Hexavalent chromium review: Part 1 Health effects, regulations, and analysis. *Journal American Water Works Association 104*, 348-357. DOI: 10.5942/jawwa.2012.104.0091

McNeill, L.S., McLean, J.E., Parks, J.L., Edwards, M.A. (2012). Hexavalent chromium review: Part 2 Chemistry, occurrence, and treatment. *Journal American Water Works Association 104*, 395-405. DOI: 10.5942/jawwa.2012.104.0092

Medvidović, N.V., Perić, J., Trgo, M., Mužek, M.N. (2007). Removal of lead ions by fixed bed of clinoptilolite-the effect of flow rate. *Microporous and Mesoporous Materials 105*, 298-304. DOI: 10.1016/j.micromeso.2007.04.015

Minitab 17.1 Statistical Software, version 17.1; Minitab, Inc.: State College, PA, USA, 2013.

Miretzky, P., Fernandez, C.A. (2010). Cr (VI) and Cr (III) removal from aqueous solution by raw and modified lignocellulosic materials: A review. *Journal of Hazardous Materials 180*, 1-19. DOI: 10.1016/j.hazmat.2010.04.060

Mondal, M.K. (2009). Removal of Pb (II) ions from aqueous solution using activated tea waste: Adsorption on a fixed-bed column. *Journal of Environmental Management 90*, 3266-3271. DOI: 10.1016/j.jenvman.2009.05.025

Owlad, M., Aroua, M.K., Daud, W.A.W., Baroutian, S. (2009). Removal of hexavalent chromium-contaminated water and wastewater: A review. *Water, Air, and Soil Pollution 200*, 59-77. DOI: 10.1007/s11270-008-9893-7

Ozdes, D., Gundogdu, A., Kemer, B., Duran, C., Kucuk, M., Soylak, M. (2014). Assessment of kinetics, thermodynamics and equilibrium parameters of Cr (VI) biosorption onto Pinus brutia Ten. *Canadian Journal of Chemical Engineering 92*, 139-147. DOI: 10.1002/cjce.21820

Paredes-Carrera, S. P., Valencia-Martínez, R. F., Valenzuela-Zapata, M. A., Sanchez-Ochoa, J. C., Castro-Sotelo, L. V. (2015). Study of hexavalent chromium sorption by hydrotalcites synthesized using ultrasound vs microwawe irradiation. *Revista Mexicana de Ingeniería Química 14*, 429-436.

Park, D., Lim, S.R., Yun, Y.S., Park, J.M. (2008). Development of a new Cr (VI)-biosorbent from agricultural biowaste. *Bioresource Technology 99*, 8810-8818. DOI: 10.1016/j.biortech.2008.04.042

Pechova, A., Pavlata, L. (2007). Chromium as an essential nutrient: A review. *Veterinarni Medicina 52*, 1-18.

Pinheiro do Prado, A.C., Manion, B.A., Seetharaman, K., Deschamps, F.C., Barrera Arellano, D.B., Block, J.M. (2013). Relationship between antioxidant properties and chemical composition of the oil and the shell of pecan nuts [*Carya illinoinensis* (Wangenh) C. Koch]. *Industrial Crops and Products 45*, 64-73.

Puică, N.M., Pui, A., Florescu, M. (2006). FTIR spectroscopy for the analysis of vegetable tanned ancient leather. *European Journal of Science and Theology 2*, 49-53.

SAS 9.2. Statistical analysis system, version 9.2; SAS Institute, Inc.: Cary, NC: 2007.

Shahbazi, A., Younesi, H., Badiei, A. (2011). Functionalized SBA-15 mesoporous silica by melamine-based dendrimer amines for adsorptive characteristics of Pb (II), Cu (II) and Cd (II) heavy metal ions in batch and fixed bed column. *Chemical Engineering Journal 168*, 505-518. DOI:10.1016/jcej.2010.11.053

Singleton, V.L., Orthofer, R., Lamuela-Raventós, R.M. (1999). Analysis of total phenols and other oxidations substrates and antioxidants by means of Folin-Ciocalteu reagent. *Methods in Enzymology 299*, 152-178. DOI: 10.1016/S0076-6879(99)99017-1

Suresh, G. (2010). Experimental investigations and theoretical modeling aspects in column studies for removal of Cr (VI) from aqueous solutions using activated tamarind seeds. *Journal of Water Resource and Protection 2*, 706-716. DOI: 10.4236/jwarp.2010.28081

Vijayaraghavan, K., Jegan, J., Palanivelu, K., Velan, M. (2005). Batch and column removal of copper from aqueous solution using a brown marine alga Turbinaria ornata. *Chemical Engineering Journal 106*, 177-184. DOI:10.1016/j.cej.2004.12.039

Wang, X.S., Li, Z.Z., Tao, S.R. (2009). Removal of chromium (VI) from aqueous solution using walnut hull. *Journal of Environmental Management 90*, 721-729. DOI: 10.1016/j.jenvman.2008.01.011

Yang, H., Yan, R., Chen, H., Lee, D. H., Zheng, C. (2007). Characteristics of hemicellulose, cellulose and lignin pyrolysis. *Fuel 86*, 1781-1788. DOI: 10.1016/j.fuel.2006.12.013

Yazaky, Y.R., Gu, Y., Lin, W., Chen, K., Nguyen, N. (1993). Analysis of black wattle (*Acacia mearnsii*) tannins-Relationships among the hide-power, the Stiasny and the ultraviolet (uv) methods. *Holzforschung 47*, 57-61. DOI: 10.1515/hfsg.1993.47.1.57

Yipmantin, A., Maldonado, H.J., Ly, M., Taulemesse, J.M., Guibal, E. (2011). Pb(II) and Cd(II) biosorption on Chondracanthus chamissoi (a red alga). *Journal of Hazardous Materials 185*, 922-929. DOI: 10.1016/j.jhazmat.2010.09.108

Zheng, X., Li, B., Zhu, B., Kuang, R., Kuang, X., Xu, B., Ma, M. (2010). Crayfish carapace micro-powder (CCM): A novel and efficient adsorbent for heavy metal ion removal from wastewater. *Water 2*, 257-272. DOI: 10.3390/w2020257